

Voltage-controlled spin injection with an endohedral fullerene Co@C₆₀ dimer

Alireza Saffarzadeh^{1,2,*} and George Kirczenow²

¹*Department of Physics, Payame Noor University, P.O. Box 19395-3697 Tehran, Iran*

²*Department of Physics, Simon Fraser University, Burnaby, British Columbia, Canada V5A 1S6*

(Dated: Wednesday 1st May, 2013)

Spin-dependent transport through an endohedral fullerene Co@C₆₀ dimer with gold electrodes is explored theoretically using density functional and extended Hückel theory. Density of states spin polarizations up to 95%, due to spin-splitting of Co 3d orbitals, are found by varying the gate and/or bias voltage. The current-voltage characteristics and strong (up to 100%) spin polarization of the current indicate that the device can be utilized for highly efficient spin injection into nonmagnetic conductors. This finding opens the way to the realization of electrostatically tuned spintronic nano devices less than 2 nanometers in size, without ferromagnetic electrodes.

Carbon-based nanostructures such as fullerenes, carbon nanotubes (CNTs), and graphene, are promising candidates for spintronic applications because of their weak spin-orbit coupling and hyperfine interaction which lead to long spin coherence lengths [1, 2]. In particular, the fullerene C₆₀ molecule is an interesting carbon nanostructure that can be used as a molecular bridge in magnetic tunnel junctions due to its remarkable structural stability and electronic properties [3, 4].

One way to generate a spin-polarized charge current is to encapsulate magnetic atoms or magnetic nanowires in fullerenes or CNTs [5–20]. For example, *ab initio* calculations showed that Co atoms in CNTs can provide strong spin polarization and considerable magnetic moments [5]. The electrical and magnetic properties of C₆₀-Co nanocomposites have also been studied [7, 11, 12] and tunnel magnetoresistance ratios up to about 30% at low bias voltages were reported, indicating significant spin polarizations [7]. Recent density functional theory (DFT) studies of encapsulated Co atoms in C₆₀ molecules [18] found hybridization between Co and C₆₀ orbitals and the most stable structure of Co@C₆₀ to have the Co atom on top of a hexagonal face. Lu *et al.* [19] showed that, in the most stable structure of Gd@C₆₀, the Gd ion is over a hexagonal ring of the C₆₀ molecule and the Gd atomic orbitals to hybridize with the C₆₀ molecular orbitals. Moreover, strong hybridization between the Gd 5d and 6s and carbon orbitals in Gd@C₆₀ has been observed, both theoretically and experimentally [20].

Magnetic atoms encapsulated in carbon nanocages, like the C₆₀ molecule, are effectively protected against environmental effects such as oxidation, stabilizing the encapsulated magnetic atoms for potential applications for spin injection in nanoscale devices. Accordingly, one can propose magnetic nano junctions to produce high spin-polarized currents with long spin coherence lengths [21]. In this paper we explore theoretically the possibility of such molecular magnetic junctions in which the carbon nanocage is a fullerene dimer. Since, among various types

of fullerene dimers, C₁₂₀ in which the two C₆₀ molecules are connected by a cyclic C₄ unit, is the simplest one and has the lowest energy as well as interesting physical and chemical properties [22], we have chosen this isomer of the C₆₀ dimer in our calculation. We note that, the electronic transport properties of a pure C₆₀ dimer [23], N and B doped C₆₀ dimer [24], and Li@C₆₀ dimer [25] have been reported theoretically, however, encapsulation of magnetic atoms in fullerene dimers has not been addressed in the previous theories.

We consider an endohedral fullerene Co@C₆₀ dimer contacted via single gold atoms (as in some experimentally realized single-molecule electronic devices [26, 27]) by semi-infinite non-magnetic electrodes, as shown in Fig. 1. The electronic density of states, degree of spin polarization, spin-polarized charge currents and differential conductances for electron tunneling through Au/Co@C₆₀-dimer/Au junction as a function of bias and gate voltage in the dimer ground state, which we find to be ferromagnetic, are studied by means of DFT calculations of the relaxed geometry and the extended Hückel model of quantum chemistry [26, 28, 29]. The extended Hückel theory (EHT) has been used to study spin transport in non-magnetic molecules contacted by magnetic electrodes [30–32] and in single molecule magnets coupled to the non-magnetic electrodes [33, 34]. However, the EHT does not by itself take account of spin polarization effects, and for this purpose we generalized the theory to include spin splittings calculated within DFT.

We carried out *ab initio* DFT geometry relaxations for the Co@C₆₀ dimer sandwiched between two Au atoms using the GAUSSIAN 09 package with the B3PW91 functional and the Lanl2DZ basis [35, 36]. In the relaxed structure (Fig. 1) the Co atoms are at off-center positions in the C₆₀ molecules, with a shortest Co-C bond length of 2.09 Å. We found the molecules to couple to each other by parallel bonds with a length of 1.59 Å in agreement with previous studies [24, 25, 37]. The Au-C and Co-Co distances are 2.26 Å and 10.49 Å, respectively. In Fig. 1, the distance between leftmost and rightmost carbon atoms is 16.31 Å. Thus our proposed spin-injection device has a size less than 2 nanometers.

The dimer system in the presence of gold electrodes is

* Author to whom correspondence should be addressed. Electronic mail: asaffarz@sfu.ca

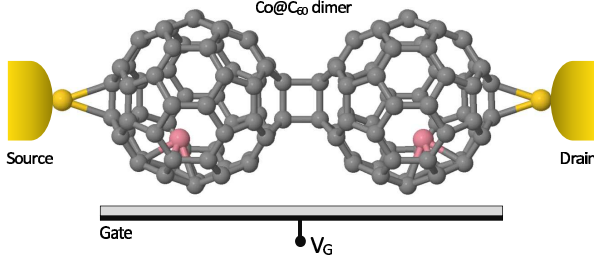


FIG. 1. (Color online) The relaxed geometry of an endohedral fullerene Co@C₆₀ dimer junction. The gray, pink, and yellow spheres represent C, Co, and Au atoms, respectively. The effect of the gate voltage, V_G , is to shift the molecular orbitals relative to the Fermi level of the gold electrodes.

described by a tight-binding model Hamiltonian derived from EHT in a basis of atomic valence orbitals, the $3d$, $4s$, and $4p$ valence orbitals of the Co atoms and the $2s$ and $2p$ orbitals of the carbon atoms. These 498 atomic orbitals form the basis set for the Co@C₆₀ dimer Hamiltonian that can be written for an electron with spin σ as

$$H_{D,\sigma} = \sum_{\alpha} \epsilon_{\alpha\sigma} d_{\alpha\sigma}^{\dagger} d_{\alpha\sigma} + \sum_{\alpha,\beta} \gamma_{\alpha\beta,\sigma} (d_{\alpha\sigma}^{\dagger} d_{\beta\sigma} + \text{h.c.}) , \quad (1)$$

where $d_{\alpha\sigma}^{\dagger}$ is the creation operator for an electron in an atomic valence orbital $\psi_{\alpha\sigma}$ with energy eigenvalue $\epsilon_{\alpha\sigma}$. $\gamma_{\alpha\beta,\sigma}$ is the spin-dependent matrix element of the extended Hückel Hamiltonian between valence orbitals $\psi_{\alpha\sigma}$ and $\psi_{\beta\sigma}$. Since the basis set used in EHT is nonorthogonal, the orbital overlap $S_{\alpha\beta,\sigma} = \langle \psi_{\alpha\sigma} | \psi_{\beta\sigma} \rangle$ that we obtain from EHT can be non-zero. Therefore, we replace $\gamma_{\alpha\beta,\sigma}$ in the Hamiltonian by $\gamma_{\alpha\beta,\sigma} - \epsilon S_{\alpha\beta,\sigma}$ where ϵ is the electron energy [38, 39]. The spin-dependence of $\epsilon_{\alpha\sigma}$ and $\gamma_{\alpha\beta,\sigma}$ results from the spin splittings of the $3d$ and $4s$ orbitals of the Co atoms that are estimated from DFT calculations for major peaks in the spin density of states for Co on graphene [40, 41]. We note that the spin-dependent electron scattering that arises from these exchange related spin-splittings is much stronger than that due to spin-orbit coupling. Therefore we neglect the latter in the present model. The spin splitting values modify the Co $4s$ and $3d$ orbitals on-site energies obtained from the EHT parameters. While the limitations of DFT are well known [26], the present theoretical approach has explained [41] the results of scanning tunneling spectroscopy experiments [42] on Co atoms adsorbed on graphene. Based on the Hamiltonian Eq. (1), the total Hamiltonian of the Co@C₆₀ dimer coupled to the left (L) and right (R) gold electrodes for an electron with spin σ can be written as $H_{\sigma} = H_{D,\sigma} + \Sigma_{L,\sigma} + \Sigma_{R,\sigma}$. Here, $\Sigma_{\eta,\sigma}(\epsilon) = \tau_{\eta,\sigma} g_{\eta}(\epsilon) \tau_{\eta,\sigma}^{\dagger}$ is a self-energy that describes the coupling of the dimer to the electrode η ($=L$ or R), $\tau_{\eta,\sigma}$ is the hopping matrix between electrode η and the dimer whose matrix elements are given by the EHT parameters. For Au atoms in the electrodes we use $6s$, $6p_x$, $6p_y$, $6p_z$, $5d_{x^2-y^2}$, $5d_{xy}$, $5d_{3z^2-r^2}$, $5d_{zx}$, $5d_{zy}$ atomic valence or-

bitals. Due to the nine valence orbitals for each Au atom, we model the electrodes, as in previous work [27, 31–34, 43], by nine semi-infinite one-dimensional chains of orthogonal atomic orbitals, with one orbital per site and periodicity a between orbital sites. The one-dimensional chains are decoupled from each other, i.e., there is no hopping between orbitals in different chains. Accordingly, the surface Green's function matrix for electrode η is $g_{\eta} = -(1/t) e^{ika} I$ where k is the electron wave number and I is a 9×9 unit matrix [44]. We note that, the overlap matrix S between the dimer and Au orbitals is included in the calculations. In this study, the Co $3d$ orbitals have been shifted in energy so that the average electric charge, corresponding to the two spin-up and spin-down states of each Co atom in the antiferromagnetic alignment and calculated from Eq. 1, is close to the Mulliken charge obtained from DFT using the GAUSSIAN 09 package. In addition, to locate the position of Fermi energy of the gold electrodes between the HOMO (highest occupied molecular orbitals) and LUMO (lowest unoccupied molecular orbital) energies of the Co@C₆₀ dimer, all the atomic valence orbitals of the dimer were shifted down in energy by $0.4t$ (in units of $t = 2.7$ eV), relative to their energies in the extended Hückel model.

The magnetic moments of the two Co atoms can be parallel (ferromagnetic (FM)) or antiparallel (antiferromagnetic (AF)). In the FM case, a spin-up electron travels from a majority spin state of one C₆₀ molecule, induced by its Co atom, to a majority spin state of the other C₆₀ molecule, induced by the other Co atom, while spin-down electrons travel from a minority spin to a minority spin state. In the AF alignment, electrons belonging to the majority spin state of one molecule, travel to the minority spin states of the other molecule and visa versa. To find the magnetic ground state configuration, we estimate the total ground state energy for each spin state in the magnetic alignment ξ ($=\text{FM}$ or AF) as $E_{\text{total},\sigma}^{\xi} = \sum_i E_{i,\sigma}^{\xi}$ where $E_{i,\sigma}^{\xi}$ is the i -th molecular orbital eigenenergy for σ spin state and the summation is over occupied molecular orbitals. We found the lowest total energy to correspond to the spin-up state of the FM alignment whose energy is lower than for the AF alignment by ~ 5.24 eV. Accordingly, to switch the Co@C₆₀ dimer from FM to AF alignment, a strong magnetic field is required. In the absence of a strong field, the Co@C₆₀ dimer will remain permanently in its FM state. In the present system the strong hybridization of the Co $3d$ orbitals and carbon valence states results in indirect exchange between the Co atoms (mediated by the carbon valence orbitals) that stabilizes the FM configuration that has also been reported in analogous structures [45–47]. Therefore, to study the effect of encapsulated Co atoms on electronic transport through the dimer bridge, only the FM alignment will be considered.

To calculate the spin states and the degree of spin polarization in this system, we define the spin-dependent Green's function of the Co@C₆₀ dimer coupled to the gold electrodes as $G_{\sigma}(\epsilon) = [(\epsilon + i\delta)S_{\sigma} - H_{\sigma}]^{-1}$ where

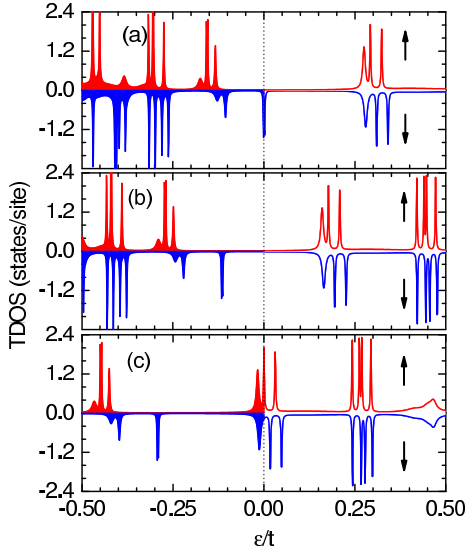


FIG. 2. (Color online) Calculated carbon atoms TDOS per site vs. electron energy ϵ for the endohedral fullerene Co@C₆₀ dimer at various gate voltages: (a) $V_G = 0.115 t/e$, (b) $V_G = 0.0 t/e$, (c) $V_G = -0.177 t/e$. The symbol \uparrow (\downarrow) corresponds to spin-up (spin-down) electrons. The vertical dotted lines indicate the position of the Fermi level. All states up to the Fermi level are occupied (shaded in the plot).

δ is a positive infinitesimal. Then the total density of states (TDOS) of carbon atoms per site for spin σ is $D_\sigma(\epsilon) = -\frac{1}{N\pi} \sum_{\alpha} \text{Im}(\langle \alpha, \sigma | G_\sigma S_\sigma | \alpha, \sigma \rangle)$, where the sum is over the carbon $2s$, $2p_x$, $2p_y$, and $2p_z$ orbitals, and $N = 120$ is the number of carbon atoms in the dimer. The degree of density of states spin polarization P is defined as $P = (D_\uparrow(E_F) - D_\downarrow(E_F)) / (D_\uparrow(E_F) + D_\downarrow(E_F))$, where $D_\uparrow(E_F)$ ($D_\downarrow(E_F)$) represents the TDOS of spin-up (spin-down) electrons at the Fermi energy. Note that, the spin dependence of electronic states at the sites of carbon atoms originates from hybridization between carbon orbitals and Co $4s$ and $3d$ orbitals. To see the effect of this hybridization on the electronic states, we show in Fig. 2 the TDOS as a function of electron energy for representative gate voltages $V_G = +0.115$, 0.0 , and $-0.177 t/e$. In our calculations, the extended Hückel model parameters describing both the on-site and intersite Hamiltonian matrix elements are recalculated for each value of the gate voltage. The dependence of the intersite Hamiltonian matrix elements on the gate voltage (see Ref. 30, Appendix A) implies that hybridization between the orbitals on different atoms depends on the gate voltage in the present theory. However, since the same gate potential is applied to the C₆₀ molecules and Co atoms, the molecular orbital features shift nearly rigidly under gating. The chosen positive and negative gate voltage values in Fig. 2 correspond to the first peaks (in the absolute value of P in the positive and negative region of gate voltage) crossing the Fermi level (see the arrows in Fig. 3). At zero gate voltage the Fermi level is located in the HOMO-LUMO gap where no molecular orbital is avail-

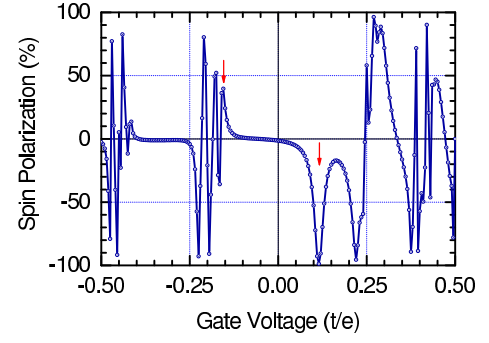


FIG. 3. (Color online) Degree of density of states spin polarization P at the Fermi energy as a function of gate voltage. The arrows show the positions of the first maxima of spin polarization with varying gate voltage.

able for electrons to tunnel through the dimer (see Fig. 2(b)), and hence little or no spin polarization is expected. By applying a gate voltage, the encapsulated Co atoms are ionized due to the gate-induced shift in energy of the molecular orbitals relative to the gold electrode's Fermi energy. The effects of the positive and the negative gate voltage, have been shown in Fig. 2(a) and 2(c), respectively. Comparing Fig. 2(b) with Fig. 2(a) and 2(c), it is clear that a positive (negative) gate voltage shifts the molecular orbitals to a higher (lower) energy and for the value of $V_G = +0.115 t/e$ at which the spin down states are conductive, there is a significant difference between the two spin populations which can cause a strong spin polarization at the Fermi level as shown in Fig. 3. On the other hand, in the case of $V_G = -0.177 t/e$ the molecular orbitals shift to a lower energy and, as shown in Fig. 3, a peak in the spin polarization appears. The results shown in Fig. 3 for P versus V_G indicate that the spin injection can be controlled by changing the gate voltage and positive or negative values for the spin polarization may be obtained, depending on the value and the sign of gate potential. The magnitude of P can exceed 90% for certain values of gate voltage which is considerably higher than that calculated for Co-nanowire@CNT (66%) [5] and those measured for Co-cluster/C₆₀ mixtures (70%) [7], Co-nanoparticle/Co-C₆₀ compounds (40%) [11] and Co crystals (42%) [48].

To investigate coherent charge transport through the Co@C₆₀ dimer, we make use of the Landauer-Büttiker formula based on the nonequilibrium Green's function method [44] for which the spin-polarized charge current at a constant bias voltage, V_b , is calculated as

$$I_\sigma(V_b) = \frac{e}{h} \int_{-\infty}^{\infty} T_\sigma(\epsilon, V_b) [f(\epsilon - \mu_L) - f(\epsilon - \mu_R)] d\epsilon, \quad (2)$$

where $f(\epsilon)$ is the Fermi function, $\mu_{L,R} = \epsilon_F \pm \frac{1}{2}eV_b$ are the chemical potentials of the electrodes, $T_\sigma = \text{Tr}[\Gamma_{L,\sigma} G_\sigma \Gamma_{R,\sigma} G_\sigma^\dagger]$ is the spin-dependent transmission function for electron tunneling through the dimer, and $\Gamma_{\eta,\sigma} = -2 \text{Im}(\Sigma_{\eta,\sigma})$ is the coupling matrix between the

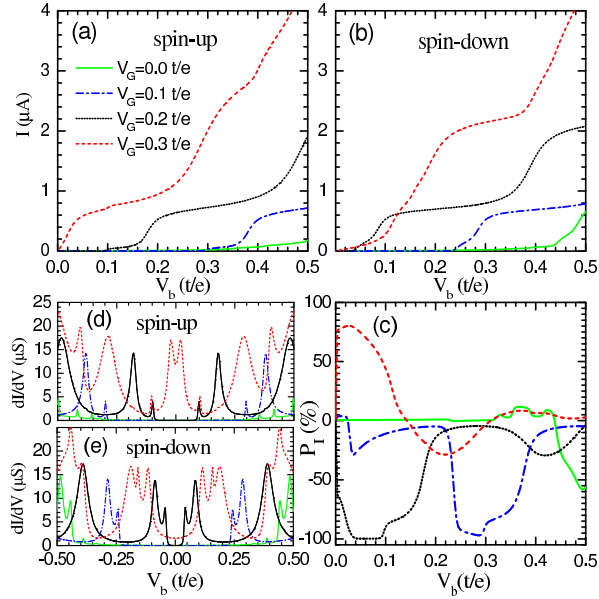


FIG. 4. (Color online) Calculated spin-dependent electric currents [(a), (b)], current spin polarization P_I (c), and differential conductances [(d), (e)] vs bias voltage for the Au/Co@C₆₀-dimer/Au junction, shown in Fig. 1, at various V_G values.

dimer and the electrode η .

The calculated current-voltage characteristics, I - V , and the differential conductance spectra, dI/dV , of the Au/Co@C₆₀-dimer/Au junction as functions of bias voltage V_b at $V_G = 0.0, 0.1, 0.2$, and $0.3 t/e$ and at temperature $T = 4.2$ K for spin-up and spin-down electrons are shown in Fig. 4. Due to the structural symmetry in the system, we obtained a symmetrical behavior in the I - V curves with respect to $V_b = 0.0 t/e$. Therefore, the results for negative bias voltages are not shown in Fig. 4(a) and 4(b). The spin up and spin down charge currents show a step-like behavior due to the entry of molecular orbitals into the bias window. The sharpness of the steps depends on the hybridization of the dimer electronic states shown in Fig. 2 to the gold electrode orbitals. The broadening of the quantized states in the scattering region causes smooth steps in the I - V curves for both spin directions. We see that the I - V characteristics of the Co@C₆₀ dimer reveal a conducting or semiconducting behavior depending on the value of gate and bias voltages. This electronic property is strongly spin dependent due to the spin splitting of Co $3d$ orbitals [40, 41] around the Fermi energy of gold electrodes. This is consistent with the work of Xie *et al.* [17] who found that hybridization between Co $3d$ and C $2p$ orbitals for Co nanowires encapsulated in CNTs is strong and results in spin polarization that increases with increasing thickness of the nanowire.

At $V_G = 0.0, 0.1$, and $0.2 t/e$, a threshold voltage that is different for spin-up and spin-down electrons, is needed to generate a charge current through the device. That is, at low gate voltages for low bias voltages the device is in

an off state, while at $V_G = 0.3 t/e$, the device is turned on and the charge current increases linearly, indicating Ohmic behavior at low biases. Such a behavior is reasonable because in this situation, the gate voltage shifts the molecular orbitals within the bias window and more channels for tunneling electrons through the Co@C₆₀ dimer bridge become accessible. Furthermore, by comparing the charge currents in Fig. 4(a) and 4(b) at each bias voltage, one can readily confirm that the tunneling channels for spin-up and spin-down electrons are well separated due to the presence of Co atoms inside the dimer. Thus, our model predicts gate and bias voltage-controlled switching between off and on states and also between spin-up and spin-down electric currents. In addition, the results shown in Fig. 4(a) and 4(b) reveal that the encapsulation of Co atoms in fullerene cages is an efficient way for injecting spin-polarized electrons into a nonmagnetic conductor by electric current. To estimate the spin injection efficiency in our model, we calculate the current spin polarization defined as $P_I = (I_\uparrow - I_\downarrow)/(I_\uparrow + I_\downarrow)$ for each bias and gate voltage. The results for P_I as a function of V_b are shown in the Fig. 4(c). We clearly see that very high values for current spin polarization ($\sim 99\%$) can be obtained in this hybrid structure. These values depend strongly on the bias and gate voltages and predict that highly efficient voltage-controlled spin injection can be achieved using the Co@C₆₀ dimer.

The differential conductances shown in Fig. 4(d) and (e) clarify the role of gate and bias voltages in controlling the spin-polarized transport through the system. To show the conductance gap, i.e., the voltage width of the zero-conductance region, we have plotted the dI/dV spectra for both positive and negative bias voltages. In Fig. 4(d) and (e) the size of the conductance gap decreases and the system gradually moves into a conducting state with increasing V_G . The symmetry of the differential conductances about $V_b = 0$ confirms the existence of symmetry in the I - V curves of Fig. 4(a) and (b). The sharp conductance peaks correspond to the step-like features seen in the I - V curves and signal the opening of new conducting channels through the dimer.

In conclusion, we have shown, based on *ab initio* and semi-empirical calculations, that very high degrees of spin polarization can be achieved for electrons tunneling through endohedral fullerene Co@C₆₀ dimers in their ferromagnetic ground state. Our results for spin-dependent I - V curves and dI/dV spectra, calculated by means of Landauer-Büttiker theory, show that these hybrid structures can be utilized for highly efficient spin injection into a nonmagnetic conductor by adjusting gate and/or bias voltages. This *electrostatic* activation should lend itself to integration of such nano spin injectors with conventional nano electronic devices. Also, since magnetic electrodes are not required to achieve spin injection in this system, the size of the device required for spin injection is that of the Co@C₆₀ dimer itself, i.e., less than 2 nanometers. Therefore as well as being of fundamental interest, systematic experimental studies of encapsu-

lated magnetic atoms in the fullerene dimer based on these findings may be relevant for nanoelectronic and

spintronic applications.

This work was supported by NSERC, CIFAR, West-Grid, and Compute Canada.

-
- [1] A.R. Rocha, V.M. Garcia-suarez, S.W. Bailey, C.J. Lambert, J. Ferrer and S. Sanvito, *Nature Materials* **4**, 335 (2005).
- [2] S. Sanvito, *Nature Nanotechnology* **2**, 204 (2007).
- [3] S. Braun, W.R. Salaneck, M. Fahlman, *Adv. Mater.* **21**, 1450 (2009).
- [4] M. Koleini and M. Brandbyge, *Beilstein J. Nanotechnol.* **3**, 589 (2012).
- [5] C.K. Yang, J. Zhao, and J.P. Lu, *Phys. Rev. Lett.* **90**, 257203 (2003).
- [6] Y. Yagi, T. M. Briere, M.H.F. Sluiter, V. Kumar, A.A. Farajian, and Y. Kawazoe, *Phys. Rev. B* **69**, 075414 (2004).
- [7] H. Zare-Kolsaraki and H. Micklitz, *Eur. Phys. J. B* **40**, 103 (2004).
- [8] N. Fujima and T. Oda, *Phys. Rev. B* **71**, 115412 (2005).
- [9] Y.-J. Kang, J. Choi, C.-Y. Moon, and K.J. Chang, *Phys. Rev. B* **71**, 115441 (2005).
- [10] S. Sakai, K. Yakushiji, S. Mitani, I. Sugai, K. Takanashi, H. Naramoto, P.V. Avramov, V. Lavrentiev, K. Narumi, Y. Maeda, *Mat. Trans.* **48**, 754 (2007).
- [11] S. Sakai, K. Yakushiji, S. Mitani, K. Takanashi, H. Naramoto, P.V. Avramov, K. Narumi, V. Lavrentiev, Y. Maeda, *Appl. Phys. Lett.* **89**, 113118 (2006).
- [12] S. Miwa, M. Shiraishi, S. Tanabe, M. Mizuguchi, T. Shinjo, and Y. Suzuki, *Phys. Rev. B* **76**, 214414 (2007).
- [13] V.V. Ivanovskaya, C. Köhler, and G. Seifert, *Phys. Rev. B* **75**, 075410 (2007).
- [14] B. Wang, Y. Zhu, W. Ren, J. Wang, and H. Guo, *Phys. Rev. B* **75**, 235415 (2007).
- [15] J.-H. Parq, J. Yu, and G. Kim, *J. Chem. Phys.* **132**, 054701 (2010).
- [16] I. Sugai, S. Sakai, Y. Matsumoto, H. Naramoto, S. Mitani, K. Takanashi, Y. Maeda, *J. Appl. Phys.* **108**, 063920 (2010).
- [17] Y. Xie, J.M. Zhang, and Y.P. Huo, *Eur. Phys. J. B* **81**, 459 (2011).
- [18] R. E. Estrada-Salas, A. A. Valladares, *J. Mol. Struct. (Theochem)* **869**, 1 (2008).
- [19] J. Lu, W.N. Mei, Y. Gao, X.C. Zeng, M. Jing, G. Li, R. Sabirianov, Z. Gao, L. You, J. Xu *et al.*, *Chem. Phys. Lett.* **425**, 82 (2006).
- [20] R.F. Sabirianov, W.N. Mei, J. Lu, Y. Gao, X.C. Zeng, R. D. Bolskar, P. Jeppson, N. Wu, A.N. Caruso, and P.A. Dowben, *J. Phys.: Condens. Matter* **19**, 082201 (2007).
- [21] K. Tsukagoshi, B. W. Alphenaar, and H. Ago, *Nature*, **401**, 572 (1999).
- [22] J.L. Segura and N. Martin, *Chem. Soc. Rev.*, **29**, 13 (2000).
- [23] J. He, K.-Q. Chen, and Chang Q. Sun, *AIP Advances* **2**, 012137 (2012).
- [24] X.H. Zheng, X.L. Wang, Z.X. Dai, and Z. Zeng, *J. Chem. Phys.* **134**, 044708 (2011).
- [25] P. Zhao, D.S. Liu, Y. Zhang, Y. Su, H.Y. Liu, S.J. Li, and G. Chen, *J. Phys. Chem. C* **116**, 7968 (2012).
- [26] For a recent review, see G. Kirczenow, in *The Oxford Handbook of Nanoscience and Technology, Volume I: Basic Aspects*, edited by A. V. Narlikar and Y. Y. Fu, Chap. 4 (Oxford University Press, Oxford, 2010).
- [27] F. Demir and G. Kirczenow, *J. Chem. Phys.* **134**, 121103 (2011); *J. Chem. Phys.* **136**, 014703 (2012).
- [28] J.H. Ammeter, H.B. Buerger, J.C. Thibeault, and R. Hoffmann, *J. Am. Chem. Soc.* **100**, 3686 (1978).
- [29] The YAEHMOP code implementation of the EHT (Ref. [28]) by G. A. Landrum and W. V. Glassey (SourceForge, Fremont, CA, 2001) was used. YAEHMOP does not include spin effects.
- [30] E.G. Emberly and G. Kirczenow, *Chem. Phys.* **281**, 311 (2002).
- [31] H. Dalgleish and G. Kirczenow, *Phys. Rev. B* **72**, 184407 (2005).
- [32] H. Dalgleish and G. Kirczenow, *Phys. Rev. B* **73**, 235436 (2006).
- [33] F. Rostamzadeh Renani and G. Kirczenow *Phys. Rev. B* **84**, 180408(R) (2011).
- [34] F. Rostamzadeh Renani and G. Kirczenow *Phys. Rev. B* **85**, 245415 (2012).
- [35] M. J. Frisch, G. W. Trucks, H. B. Schlegel, G. E. Scuseria, M. A. Robb, J. R. Cheeseman, G. Scalmani, V. Barone, B. Mennucci, G. A. Petersson *et al.*, the Gaussian 09 Revision: A.02 computer code was used.
- [36] J. P. Perdew, K. Burke, and M. Ernzerhof, *Phys. Rev. Lett.* **77**, 3865 (1996).
- [37] A. Trave, F.J. Ribeiro, S. G. Louie, and M. L. Cohen, *Phys. Rev. B* **70**, 205418 (2004).
- [38] E. Emberly and G. Kirczenow, *Phys. Rev. Lett.* **81**, 5205 (1998).
- [39] E. Emberly and G. Kirczenow, *J. Phys. Condens. Matter* **11**, 6911 (1999).
- [40] K.T. Chan, H. Lee, and M.L. Cohen, *Phys. Rev. B* **83**, 035405 (2011).
- [41] A. Saffarzadeh and G. Kirczenow, *Phys. Rev. B* **85**, 245429 (2012).
- [42] V.W. Brar, R. Decker, H. Solowan, Y. Wang, L. Maserati, K.T. Chan, H. Lee, C.O. Girit, A. Zettl, S.G. Louie *et al.*, *Nat. Phys.* **7**, 43 (2011).
- [43] D. M. Cardamone and G. Kirczenow, *Phys. Rev. B* **77**, 165403 (2008).
- [44] S. Datta, *Quantum Transport: Atom to Transistor* (Cambridge University Press, Cambridge, 2005).
- [45] X. Xu and H. S. Kang, *J. Chem. Phys.* **128**, 074707 (2008).
- [46] R. Xiao, D. Fritsch, M. D. Kuźmin, K. Koepernik, H. Eschrig, M. Richter, K. Vietze and G. Seifert, *Phys. Rev. Lett.* **103**, 187201 (2009).
- [47] R. Robles and S. N. Khanna, *J. Chem. Phys.* **130**, 164313 (2009).
- [48] R.J. Soulen Jr., J.M. Byers, M.S. Osofsky, B. Nadgorny, T. Ambrose, S.F. Cheng, P.R. Broussard, C. T. Tanaka, J. Nowak, J. S. Moodera *et al.*, *Science* **282**, 85 (1998).